



Full length article

Re-evaluation of the mechanical properties and creep resistance of commercial magnesium die-casting alloy AE44

Suming Zhu^{a,b}, Trevor B. Abbott^{a,b,c,d}, Jian-Feng Nie^b, Hua Qian Ang^a, Dong Qiu^a, Kazuhiro Nogita^d, Mark A. Easton^{a,*}

^aSchool of Engineering, RMIT University, Carlton, Victoria 3053, Australia

^bDepartment of Materials Science and Engineering, Monash University, Victoria 3800, Australia

^cMagontec Limited, Sydney, New South Wales 2000, Australia

^dSchool of Mechanical and Mining Engineering, The University of Queensland, St Lucia, Queensland 4072, Australia

Received 20 May 2020; received in revised form 11 April 2021; accepted 14 April 2021

Available online 19 June 2021

Abstract

This paper presents a re-evaluation of the room temperature mechanical properties and high temperature creep resistance of magnesium die-casting alloy AE44 (Mg-4Al-4RE) in light of the influence of minor Mn addition. It is shown that the Mn-containing AE44 exhibits distinct age hardening response upon direct ageing (T5) due to the precipitation of nanoscale Al-Mn particles, as reported previously in a similar alloy. The T5 ageing leads to a significant improvement in strength with similar ductility. Consequently, the T5-aged AE44 has a remarkably better strength-ductility combination than most Mg die-casting alloys and even the Al die-casting alloy A380. Minor Mn addition is also shown to be critical for the creep resistance of AE44 whereas the influence of the RE constituent is not as significant as previously thought, which reaffirms that precipitation hardening of the α -Mg matrix is more important than grain boundary reinforcement by intermetallic phases for the creep resistance of die-cast Mg alloys. The findings in this work could provide new application perspectives for AE44, particularly in the automotive industry.

© 2021 Chongqing University. Publishing services provided by Elsevier B.V. on behalf of KeAi Communications Co. Ltd.

This is an open access article under the CC BY-NC-ND license (<http://creativecommons.org/licenses/by-nc-nd/4.0/>)

Peer review under responsibility of Chongqing University

Keywords: Magnesium alloys; Manganese; Precipitation hardening; Mechanical properties; Creep; Die casting.

1. Introduction

There have been enormous efforts the past decades in developing magnesium die-casting alloys for elevated temperature applications, such as internal combustion engine powertrain components and power tools for forestry, gardening and construction, where excellent creep resistance and die-castability are required [1,2]. Amongst the alloys developed, one important family are those based on the Mg-Al-Rare Earth (RE) system, notably AE42 (Mg-4Al-2RE, all compositions in weight percent hereafter unless specified) and AE44 (Mg-4Al-4RE). AE42 has previously used as

a benchmark for creep-resistant Mg alloys, but its creep resistance tends to drop rapidly at temperatures above 150 °C [3] and has hot tearing issues [4]. AE44 was developed based on AE42 by adding more RE [5,6], with improved creep resistance and castability. Traditionally, RE was added in the form of misch metal, i.e. a mixture of several RE elements including Ce, La, Nd and Pr, with Ce being the most abundant element [5–9]. In recent years, the high demand for Nd in magnetic applications has made the two-element misch metal (containing only Ce and La) considerably cheaper than the four-element misch metal. Consequently, currently produced AE44 contains only Ce and La (referred to here as AE44–2) [10–13]. A thorough evaluation of AE44–2 and the former AE44 (referred to here as AE44–4), together with other commercially available high temperature Mg die-casting

* Corresponding author.

E-mail address: mark.easton@rmit.edu.au (M.A. Easton).

Table 1
Chemical composition of the die-cast AE44 alloys in this work and from the previous studies [13,19].

Alloy	Composition										Note
	Al (%)	Mn (%)	Ce (%)	La (%)	Nd (%)	Pr (%)	Zn (%)	Fe (ppm)	Si (ppm)	Be (ppm)	
AE44-0Mn	3.99	0.03	1.94	1.030	<0.005	–	0.005	–	–	–	This work
AE44-0.1Mn	3.83	0.09	2.67	1.690	<0.005	–	0.008	–	–	–	This work
AE44-0.2Mn	3.97	0.18	2.38	1.380	<0.005	–	0.008	15	340	3	This work
AE44-0.3Mn	3.67	0.31	2.5	1.330	<0.005	–	0.01	–	–	–	This work
AE44-0.4Mn	3.86	0.38	2.61	1.660	<0.005	–	0.01	–	–	–	This work
AE44-2	3.95	0.15	2.82	1.32	<0.005	–	0.014	116	260	4	[13]
AE44-4	3.73	0.30	2.47	1.21	0.51	0.1	0.012	92	260	3	[13]
ALa44	4.05	0.27	0.01	3.87	<0.005	–	0.04	70	80	3	[19]
ACe44	3.97	0.14	4.04	0.03	<0.005	–	0.008	114	410	4	[19]
ANd44	3.92	0.11	0.04	0.005	4.06	–	0.006	78	265	4	[19]

alloys, has been completed [12,13]. Amongst the alloys evaluated, AE44–2 has the best combination of material cost, die-castability and high temperature creep resistance.

The Mg-Al-RE based alloys generally exhibit superior creep resistance to the common Mg-Al based alloys such as AZ91 (Mg-9Al-1Zn) and AM60 (Mg-6Al-0.3Mn). It is well accepted that the improved creep resistance of the Mg-Al-RE alloys is due to the preferential formation of the Al-RE intermetallic phases instead of the $Mg_{17}Al_{12}$ phase that has a low melting point and tends to coarsen at elevated temperatures. However, there has been a debate on the underlying mechanism for the improvement in creep resistance of the Mg-Al-RE alloys. In some studies [6,11,14,15], the thermal stability of the Al-RE intermetallic phases was considered to play an important role in the creep resistance of the Mg-Al-RE alloys. Powell et al. [14] attributed the deterioration in creep resistance in AE42 at temperatures above 150 °C to the formation of the $Mg_{17}Al_{12}$ phase as a result of the decomposition of the $Al_{11}RE_3$ phase to the Al_2RE phase. Bakke et al. [6] attributed the better creep resistance of AE44 than AE42 to the formation of Al_2RE as the dominant intermetallic phase, assuming that it is more stable than the $Al_{11}RE_3$ phase. Zhang et al. [11,15] found that the creep performance of AE44 is affected by the choice of individual RE elements (La, Ce or Nd) and they attributed the difference in creep resistance to the thermal stability of the $Al_{11}RE_3$ phase, with $Al_{11}La_3$ being most stable, followed by $Al_{11}Ce_3$, and $Al_{11}Nd_3$ being the least stable. However, there was evidence in other studies [8,9,16–18] showing that the $Al_{11}RE_3$ phase can be stable at temperatures up to 450 °C without decomposition to the Al_2RE phase. Zhu et al. [16] attributed the deterioration in creep resistance of AE42 at temperatures above 150 °C to the precipitation of the $Mg_{17}Al_{12}$ phase from the supersaturation of Al solute in the α -Mg matrix as a result of high solidification rate in die casting. Rzychoń et al. [8] and Zhu et al. [9] ascribed the better creep resistance of AE44 over AE42 to a higher fraction of the $Al_{11}RE_3$ phase and a reduced level of Al solute in the α -Mg matrix. Zhu et al. [19] also compared the creep properties of die-cast AE44 containing different RE elements, i.e. La, Ce or Nd, and showed that the observed difference in creep resistance between these alloys cannot be accounted for by the thermal stability of the $Al_{11}RE_3$ phase. The volume

fraction of the Al-RE intermetallic phases (mainly $Al_{11}RE_3$) was suggested to be the main factor for the observed differences in creep resistance. It should be pointed out that, despite the debate on its thermal stability, the $Al_{11}RE_3$ phase was believed to be the most important microstructural factor for the creep resistance of the Mg-Al-RE alloys in these studies. Recently, Meng et al. [20] reported the development of ALaM440 (Mg-3.5Al-4.2La-0.3Mn) alloy, which shows a better strength-ductility balance and a better cost/creep resistance combination than the common Mg die-casting alloys. They attributed the better mechanical performance to the formation of η - Al_3La as the predominant intermetallic phase.

AE alloys, like other Mg-Al based alloys, normally contain 0.2–0.3% Mn as an essential ingredient to control the Fe level in the melting process to improve the corrosion resistance. It was found [21] that minor Mn additions also have a remarkable age hardening effect in die-cast Mg-4Al-3La alloy. For example, the yield strength of the Mg-4Al-3La alloy with 0.32% Mn was increased by ~30 MPa (~25%) after ageing at 200 °C for 32 h without prior solution treatment. The minor Mn additions were also found [22] to have a significant effect in improving the high temperature creep resistance of the Mg-4Al-3La alloy. Therefore, the aim of the present study is to re-evaluate the room temperature mechanical properties and high temperature creep resistance of AE44 in light of the influence of minor Mn addition. For this purpose, the age hardenability in AE44 and the effect of ageing on mechanical properties are evaluated. In addition, the creep properties of a range of die-cast AE44 alloys with various levels of Mn addition, including those in our previous studies [13,19] where the differences in creep resistance were related to the RE constituent, are analysed or re-analysed by taking into account the Mn content. The optimised mechanical properties of AE44 are compared with those of other Mg die-casting alloys and an Al die-casting alloy and new application perspectives in the automotive industry are discussed.

2. Materials and methods

The alloys evaluated in this work and their compositions (wt.%) are shown in Table 1. All alloys were cast in a 250 tonne Toshiba cold chamber high pressure die casting ma-

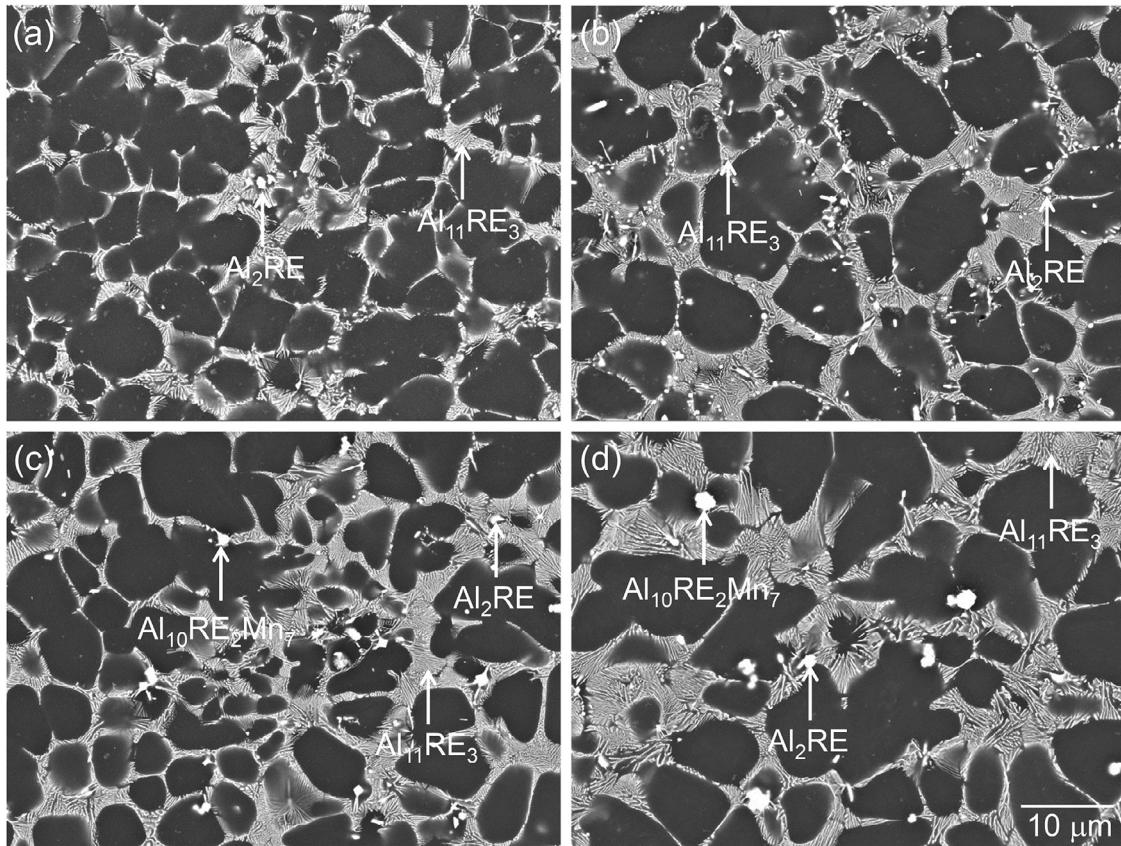


Fig. 1. SEM backscattered electron images showing as-cast microstructure in the AE44 alloys with various Mn contents: (a) AE44-0Mn, (b) AE44-0.1Mn, (c) AE44-0.2Mn and (d) AE44-0.4Mn. The intermetallic phases were identified by EDX. Note the presence of a few, coarse $\text{Al}_{10}\text{RE}_2\text{Mn}_7$ particles in the AE44-0.2Mn and AE44-0.4Mn alloys.

chine using a 3-cavity die to produce one rectangular dog-bone shaped tensile specimen (5.75 mm width and 3 mm thickness) and two cylindrical tensile bars (5.65 mm diameter). The alloy melts were produced in a resistance heated crucible and held at around 700 °C before casting. During melting and holding, the melt was protected by HFC-134a in CO_2 carrier gas. More details of alloy preparation can be found elsewhere [12].

The cylindrical tensile bars were used to evaluate mechanical properties and creep performance. The constant load creep tests were conducted at 175 °C on creep testing rigs. The creep strain was measured continuously by an extensometer that was attached directly to the specimen gauge section. The tensile tests were carried out at room temperature on a screw-driven Instron machine. The crosshead speed employed was 5 mm/min, corresponding to an initial strain rate of $2.3 \times 10^{-3} \text{ s}^{-1}$. The age hardening response was evaluated at 200, 250 and 300 °C using the rectangular dog-bone specimens, with no prior solution treatment applied. The hardness measurements were obtained under a load of 1 kg.

Scanning electron microscopy (SEM) and transmission electron microscopy (TEM), high resolution transmission electron microscopy (HRTEM) and energy dispersive X-ray (EDX) spectroscopy were used for microstructure characterisation. The foils for the TEM examinations were prepared by low-angle ion milling.

3. Results

3.1. As-cast microstructure

Fig. 1 shows the SEM backscattered electron images of the current AE44 alloys with various levels of Mn addition. The microstructure is characterised by primary α -Mg dendrites surrounded by intermetallic phases in the interdendritic/grain boundary regions. It is obvious that $\text{Al}_{11}\text{RE}_3$ is the predominant intermetallic phase for all alloys, which has a fibrous or lamellar-like morphology. Besides the $\text{Al}_{11}\text{RE}_3$ phase, minor Al_2RE phase with a particulate shape is also present in the microstructure for all alloys. With increasing Mn content, blocky $\text{Al}_{10}\text{RE}_2\text{Mn}_7$ phase can be seen in the microstructure, especially for the AE44-0.2Mn and AE44-0.4Mn alloys. Detailed characterisation of the intermetallic phases can be found in previous studies [8,9]. From the above results, it appears that, apart from introducing a small amount of the $\text{Al}_{10}\text{RE}_2\text{Mn}_7$ phase, the minor Mn additions do not have much influence on the fraction and morphology of the $\text{Al}_{11}\text{RE}_3$ and Al_2RE phases.

3.2. Age hardenability and precipitation

Changes in hardness of the AE44-0.3Mn alloy during ageing at 200, 250 and 300 °C are shown in Fig. 2. The alloy

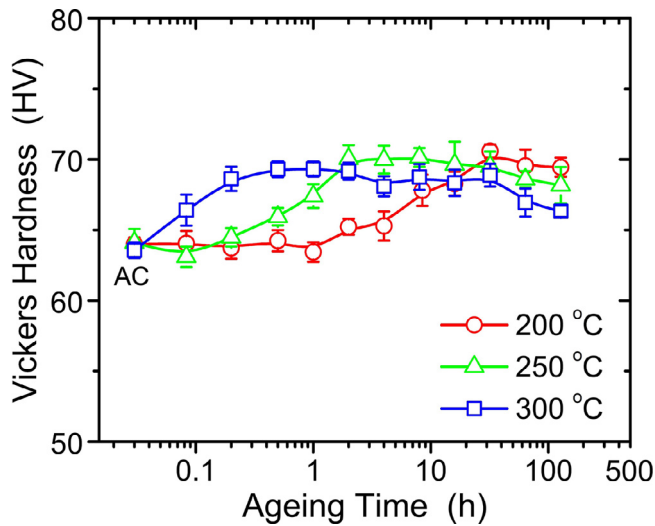


Fig. 2. Age hardening responses of the AE44-0.3Mn alloy upon ageing at various temperatures.

exhibits a distinct age hardening response for all ageing temperatures, with the time to reach the peak hardness being about 32, 4 and 1 h at 200, 250 and 300 °C, respectively. It is noted that there is only a slight decrease in hardness after reaching the peak, suggesting that the precipitates induced by ageing have relatively good thermal stability. In addition, the peak hardness only shows a marginal decrease with increasing ageing temperature, implying that the ageing temperature is not critically important for the mechanical properties.

The TEM examinations revealed the formation of nanoscale precipitates in the alloy after ageing. The TEM and HRTEM images of the precipitates in the alloy aged at 300 °C for 128 h are shown in Fig. 3. Most precipitates appear to be near spherical in shape and less than 10 nm in size. As in our previous work [21], these nanoscale precipitates are found to contain mainly Al and Mn. This is consistent with the predicted solubility limit of Mn in AE44, which will be shown later on. In addition, there have been reports on the identi-

fication of Al-Mn precipitates in Mg-Al based alloys [23–25]. Yang et al. [23] identified the nano-sized, Mn-containing precipitates in a die-cast AE44 alloy as Al_8Mn_5 with a rhombohedral structure, with a good crystallographic matching with the α -Mg matrix. Qin et al. [24] reported the presence of Al_6Mn precipitates in a die-cast ALaX431 (Mg-4Al-3La-1Ca-0.3Mn) alloy, which has orientation relationships with the η - Al_3La intermetallic phase. On the other hand, Zeng et al. [25] identified the nanoscale Al-Mn precipitates as quasicrystalline phase in a sand-cast AZ91 alloy. Work is ongoing to resolve the identity of the precipitates in the current AE44-0.3Mn alloy and the results will be published in due course.

3.3. Room temperature mechanical properties

Representative tensile curves of the AE44-0.3Mn alloy in the die-cast and peak-aged (T5) conditions are shown in Fig. 4a. For comparison, typical tensile curves of the die-cast AZ91 and AM60 in the previous study [13] are shown in Fig. 4b. Fig. 4c is an enlarged portion of Fig. 4a, showing the early stage of tensile deformation. Pronounced anelasticity is noted for the AE44-0.3Mn alloy, especially in the die-cast state. With the presence of anelasticity, the yield strength determined using the conventional 0.2% offset method is clearly underestimated. To account for the anelasticity, using a higher offset can give a more approximate estimation of yield strength than using the conventional 0.2% offset [26]. Therefore, 0.5% offset was used for the determination of yield strength in this study, as shown in Fig. 3c. The measured 0.5% yield strength, tensile strength and elongation to failure are presented in Table 2. It is apparent that the T5 ageing leads to remarkable improvements in strength for the AE44-0.3Mn alloy and the improvement is largest for the ageing at 200 °C. It is worth noting that the T5 ageing appears to have a marginal effect on ductility. As a result, the T5-aged AE44-0.3Mn alloy exhibits superior mechanical properties, with yield strength better than that of AZ91 and ductility similar to that of AM60.

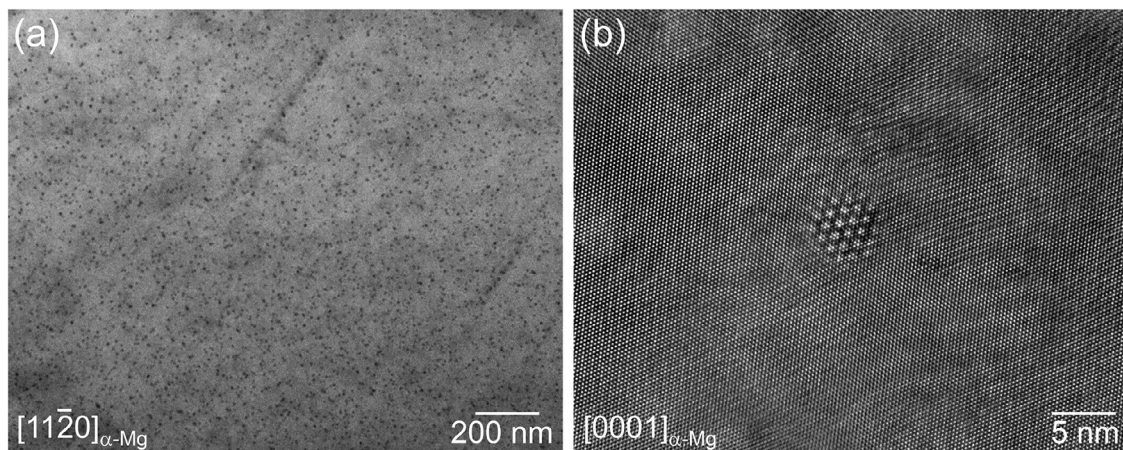


Fig. 3. Nanoscale Al-Mn precipitates in the AE44-0.3Mn alloy after ageing at 300 °C for 256 h: (a) TEM bright field image viewed along the $[11\bar{2}0]_{\alpha\text{-Mg}}$ and (b) HRTEM image viewed along the $[0001]_{\alpha\text{-Mg}}$.

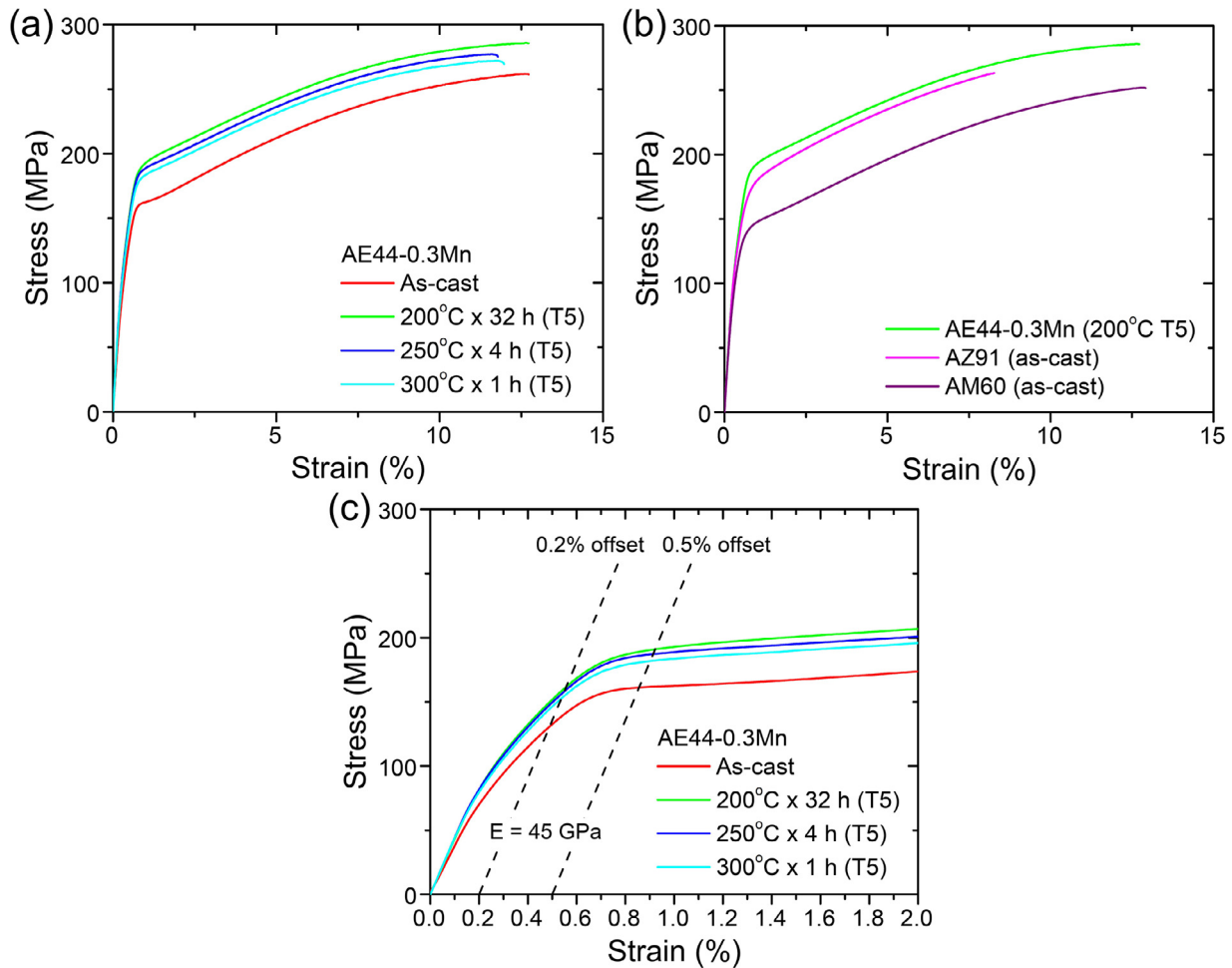


Fig. 4. Room temperature tensile test curves: (a) the AE44-0.3Mn alloy in the as-cast and various T5-aged conditions (b) the T5-aged (200 °C for 32 h) AE44-0.3Mn alloy as compared with the as-cast AZ91 and AM60 alloys [13]. (c) is an enlarged portion of (a), showing the presence of anelasticity and its influence on determination of yield strength. The 0.2% and 0.5% offsets are indicated by dashed lines with a gradient of 45 GPa in (c).

Table 2

Room temperature tensile properties of the AE44-0.3Mn alloy in the as-cast and peak-aged conditions. For comparison, the as-cast AZ91 and AM60 alloys in the previous study [13] are also included.

Alloy	Condition	0.5% Yield Strength (MPa)	Tensile Strength (MPa)	Elongation (%)
AE44-0.3Mn	as-cast	161.5 ± 0.4	258.0 ± 8.5	12.1 ± 2.3
	200 °C × 32 h	192.4 ± 1.3	284.1 ± 3.2	11.4 ± 1.6
	250 °C × 4 h	185.3 ± 1.9	275.4 ± 2.2	11.3 ± 0.7
	300 °C × 1 h	181.7 ± 0.2	273.5 ± 2.2	12.1 ± 0.4
AZ91	as-cast	178.2 ± 2.3	264.8 ± 2.7	8.2 ± 1.1
AM60	as-cast	144.3 ± 1.3	248.6 ± 7.2	12.3 ± 1.2

A comparison of mechanical properties for the T5-aged (200 °C for 32 h) AE44-0.3Mn alloy and other Mg die-casting alloys [13], together with an Al die-casting alloy (A380) [13], is shown in Fig. 5, in which yield strength is plotted against elongation to fracture. The most recently developed Mg-Al-La based die-casting alloys, including ALaM440 [20], ALaX431 (Mg-4Al-3La-1Ca-0.3Mn) [24] and ALaGd432 (Mg-4Al-3La-2Gd-0.3Mn) [27] are also included. As can be expected, a higher yield strength generally comes with a lower elongation and vice versa for these alloys. Whilst the AXJ530 alloy has relatively higher yield strength (~205 MPa) but a lower elon-

gation (~4%), the AE42 and AE44-0.3Mn, together with AS31 and AM60 tend to have higher elongations (above 10%) but relatively lower yield strengths (~145–162 MPa). However, the yield strength is increased to ~192 MPa whilst the elongation is maintained at above 10% for the AE44-0.3Mn alloy after T5 ageing. Consequently, the T5-aged AE44-0.3Mn alloy possesses a much better combination of strength and ductility compared to the Al die-casting alloy A380 and other Mg die-casting alloys except the recently developed ALaM440, ALaX431 and ALaGd432. Needless to say, if the relative density were taken into account, the margin between the T5-aged

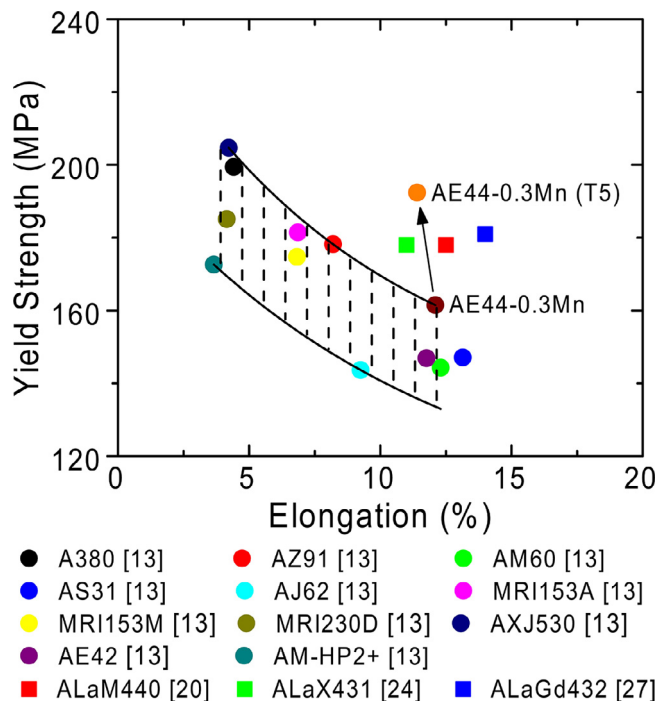


Fig. 5. 0.5% yield strength versus elongation to fracture for the as-cast and T5-aged ($200\text{ }^{\circ}\text{C} \times 32\text{ h}$) AE44-0.3Mn as compared with other die-cast Mg alloys and Al alloy A380 [13]. Also shown are the most recently developed Mg-Al-La based die-casting alloys, including ALaM440 [20], ALaX431 (Mg-4Al-3La-1Ca-0.3Mn) [24] and ALaGd432 (Mg-4Al-3La-2Gd-0.3Mn) [27].

AE44-0.3Mn alloy and the Al die-casting alloy A380 would be even greater. It is noted that all ALaM440, ALaX431 and ALaGd432 have a better combination of strength and ductility than the current AE44-0.3Mn alloy in the die-cast condition. This difference could be related to the casting conditions as the ALaM440, ALaX431 and ALaGd432 alloys were produced by hot chamber die casting using a die preheated to $\sim 240\text{ }^{\circ}\text{C}$ whilst the current AE44-0.3Mn alloy was produced by cold chamber die casting using a die without preheating. Casting the ALaM440, ALaX431 and ALaGd432 alloys into a preheated die may have induced ageing hardening during the subsequent cooling.

3.4. High temperature creep resistance

The creep curves at $175\text{ }^{\circ}\text{C}$ under a stress of 90 MPa for the current AE44 alloys with different Mn additions and other AE44 variants from previous studies [13,19] are shown in Fig. 6a–c. It is apparent that the minor Mn additions have a remarkable influence in improving creep resistance for the current AE44, with the AE44-0Mn specimen failing in less than 10 h whilst the Mn-added specimens sustained 300 h without failure. The better creep resistance exhibited by the AE44-4 as compared with the AE44-2 was previously thought to be related to the difference in RE constituent, with the former containing Nd and Pr in addition to Ce and La, but the influence of Mn content was not considered [13]. For the

ALa44, ACe44 and ANd44 alloys, the volume fraction of intermetallic phases was concluded to be the main contributing factor for the observed differences in creep resistance [19].

To better understand the influence of Mn additions on creep resistance, the minimum creep rate is plotted against the Mn content for all AE44 variants and is shown in Fig. 6d. There appears to be a good correlation between the minimum creep rate and the Mn content, especially for the current AE44 and the previous ALa44 and AE44-4, suggesting that Mn content is critical for the creep resistance of AE44 alloys, whereas the influence of the particular RE constituent is not as significant as previously thought. Given that the creep resistance of the ANd44 and ACe44 is still lower after the influence of Mn content is taken into account (comparing the ANd44 and ACe44 data points in Fig. 6d with the AE44-xMn baseline), the volume fraction of intermetallic phases does appear to have some influence on creep resistance of AE44, but it is most likely not the main contributing factor as previously reported [19]. The current results also support the use of La as the primary rare earth recently by Meng et al. [20] in the development of Mg-3.5Al-4.2La-0.3Mn (ALaM440) alloy with superior creep resistance.

4. Discussion

4.1. Age hardenability in die-cast AE44 induced by minor Mn addition

Die-cast AE44 normally contains about 0.3% Mn to improve the corrosion resistance through reducing the Fe content during the melting process. It is interesting to see that a minor Mn addition can give rise to age hardening in AE44 through T5 heat treatment. To better understand the age hardenability induced by the minor addition of Mn, the solubility limit of Mn in AE44 was calculated using PANDAT software [28] with the PanMagnesium 2018 database. For simplification, all RE in AE44 was assumed to be Ce. Fig. 7 provides information on how the Mn content in the α -Mg changes with cooling. At the start of solidification, the Mn content in α -Mg is 0.22%, which is the maximum solubility of Mn in the α -Mg matrix (the first to solidify being at the centre of the grains). The last α -Mg matrix to solidify contains only 0.07% Mn (the grain boundary regions). If the Mn content in the alloy is below 0.22%, the Mn level in the grain interior will decrease, but the Mn level at the grain boundary regions is not expected to change until the Mn content falls below 0.07%. It is noted that the solubility of Mn drops sharply with decreasing temperature and it is close to zero at $175\text{ }^{\circ}\text{C}$, which is in support of the observations that minor Mn additions lead to age hardening in AE44. From Fig. 7, the optimal Mn content for maximising age hardening should be around 0.22%. It should be pointed out that the precipitation phase is predicted to be Al_8Mn_5 according to the thermodynamic calculations, but this phase is not experimentally verified in this work (Fig. 3).

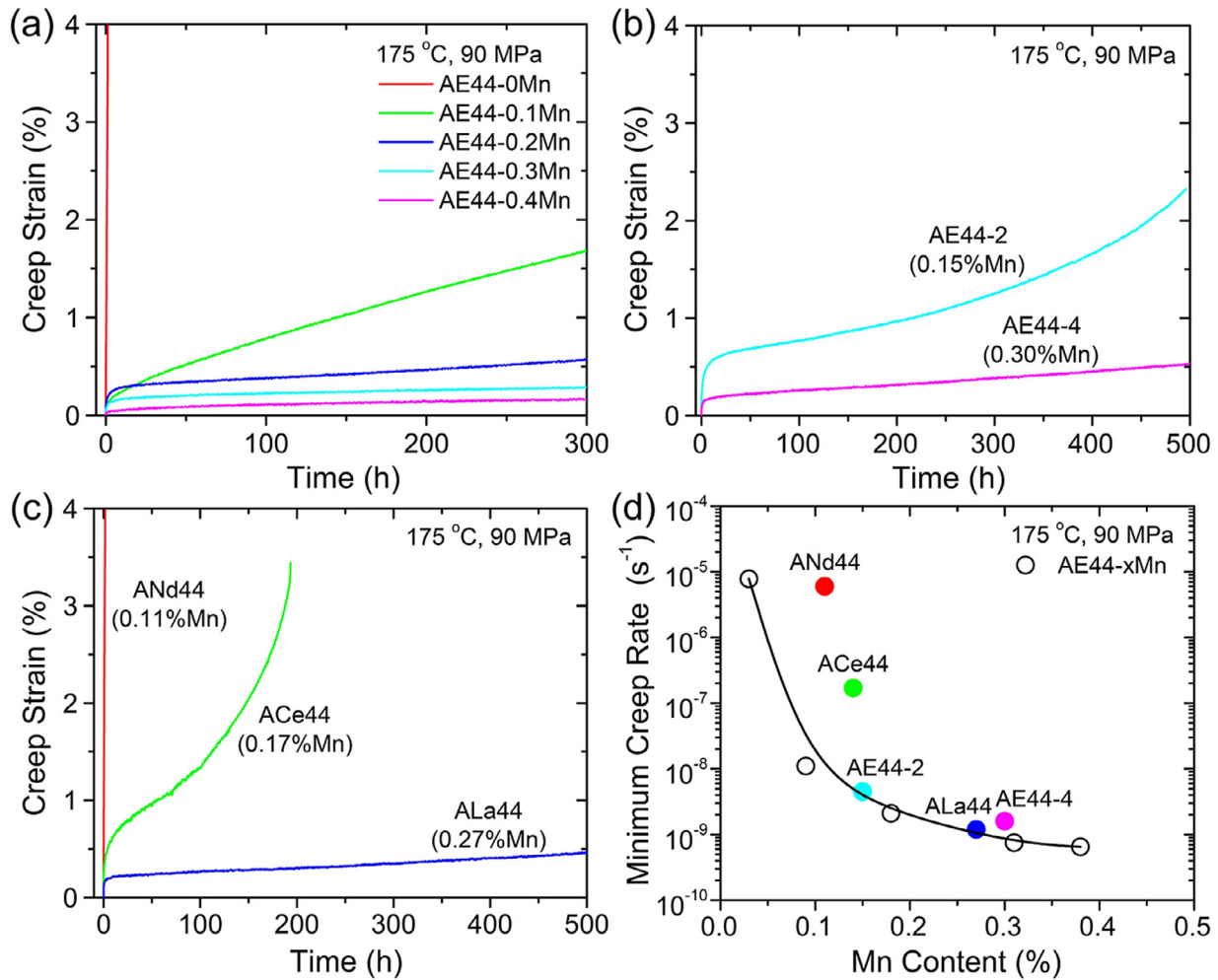


Fig. 6. Creep properties at 175 °C and 90 MPa: (a) creep curves of the AE44 alloys with various Mn contents in this work, (b) creep curves of the AE44–2 and AE44–4 [13], (c) creep curves of the ALa44, ACe44 and ANd44 [19], and (d) minimum creep rate plotted against Mn content for all AE44 variants.

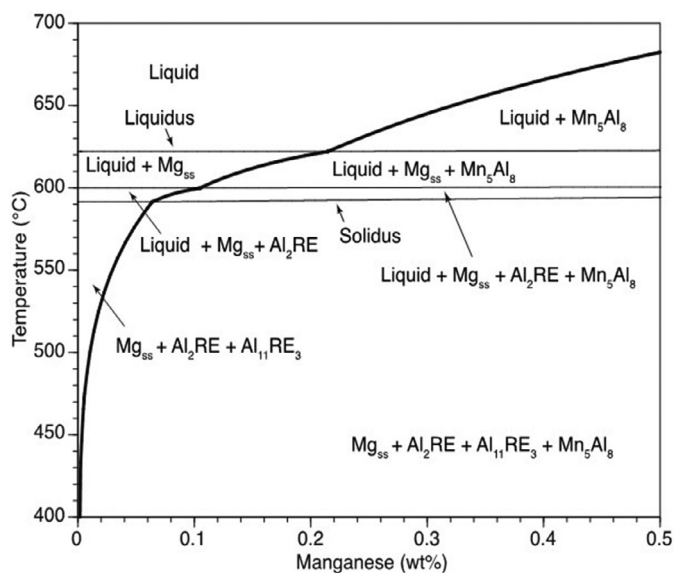


Fig. 7. Computed isopleth of Mg-4Al-4Ce phase diagram using Pandat Pan-Magnesium 2018 database showing the solubility limit of Mn.

4.2. The critical role of minor Mn in creep resistance of die-cast AE44

The superior creep resistance of die-cast AE44 as compared to AZ91 and AM60 is generally attributed to the formation of the Al-RE intermetallic phases. However, the present study indicates that it is the minor addition of Mn that plays a critical role in the creep resistance of AE44. Similar effects of minor Mn additions on creep resistance have also been reported in other Mg-Al based casting alloys, such as AJ62 [29], Mg-6Al-3Ca-0.5Mn [30], Mg-2Al-2Ca-0.3Mn [31] and MRI230 [32,33]. The improvements of creep resistance in these alloys were attributed to the formation of nanoscale Al-Mn precipitates [29,30] or ordered GP zones [31] or clusters [33]. As dislocation creep is most likely the dominant creep mechanism for die-cast AE44 [9], the effect of minor Mn on creep resistance of AE44 can be related to the precipitation hardening of nano-scale Al-Mn particles, which most likely occurs dynamically in the creep process as the dislocations produced by the creep deformation can act as heterogeneous nucleation sites. In view of the fact that the minor Mn addi-

tion has much more significant effect on creep resistance of AE44 than the volume fraction of intermetallic phases, this work reaffirms that precipitation strengthening of the α -Mg matrix is more important than grain boundary reinforcement by the intermetallic phase for the creep resistance of die-cast Mg alloys, as suggested previously [34].

The present study also indicates that the influence of the RE constituent on the creep resistance of AE44 is not as significant as previously thought. This justifies the development of low-cost AE44 that contains cheaper RE elements such as La and/or Ce, without using very expensive RE elements such as Nd and Pr.

4.3. New application perspectives

Like AE42, AE44 was originally developed as a creep-resistant Mg die-casting alloy for internal combustion engine powertrain applications where the operating temperatures can be as high as 200 °C. AE44 has been shown to be the most promising Mg die-casting alloy for the front engine cradle of automotive vehicles [35] and has found significant usage in high performance internal combustion engine based vehicles such as those produced by Porsche and Audi. However, the commercial drivers for Mg die-casting alloys in automotive industry have changed considerably over the last few years with the emergence of electric vehicles (EV), in which analogs to the internal combustion engine powertrain components do not exist. Opportunities for vehicle weight reduction are now in vehicle body structures and EV motor and battery enclosures. As a result, the property requirements for Mg die-casting alloys have shifted from creep resistance to strength-ductility combinations and thermal conductivity.

So far, AE alloys have not been considered for structural applications in vehicles because of the relatively low yield strength at room temperature, despite these alloys having excellent ductility. The relatively low yield strength of AE alloys was thought to be mainly due to the predominant $Al_{11}RE_3$ intermetallic phase having a lamellar-like structure rather than being fully divorced and forming a percolating network [13]. Intermetallic phases with profuse spatial interconnection tend to have additional strengthening effect in addition to the well-known dispersion hardening from isolated second-phase particles [36]. Another factor is the reduced level of Al solute in the α -Mg matrix, which leads to less solid solution strengthening.

It is encouraging to see that the yield strength of die-cast AE44 can be remarkably enhanced by ageing without losing too much ductility, and consequently the T5-aged AE44-0.3Mn alloy possesses a much better combination of strength and ductility than other Mg die-casting alloys and the Al die-casting alloy A380. Thus, the age hardenability in die-cast AE44 is expected to provide new perspectives in automotive structural applications such as shock towers, crash systems and space frames. Furthermore, the age hardening can be achieved in the normal coating and painting process for automotive parts, without incurring additional cost.

5. Conclusions

The room temperature mechanical properties and high temperature creep resistance of die-cast AE44 have been re-evaluated in light of the influence of minor Mn addition. The following conclusion are drawn:

- (1) Die-cast AE44 is age-hardenable upon T5 ageing owing to the precipitation of nanoscale Al-Mn particles. The T5 ageing leads to a significant improvement in strength whilst retaining similar ductility.
- (2) Minor Mn addition plays a critical role in the creep resistance of die-cast AE44, whereas the influence of the RE constituent is not as significant as previously thought. This justifies the development of low-cost AE44 that contains cheaper RE elements such as La and/or Ce.
- (3) The T5-aged AE44 has a substantially better strength-ductility combination than most Mg die-casting alloys and even the Al die-casting alloy A380. The age hardenability could provide new application perspectives for die-cast AE44, particularly in the automotive industry.

Declaration of Competing Interest

Magontec Ltd provided the AE44 alloys used in this work. Dr. Trevor Abbott is a consultant to Magontec Ltd.

Acknowledgments

This work was supported by Australian Research Council (LP160100690) and Magontec Ltd. Monash Centre for Electron Microscopy (MCEM) is acknowledged for access to experimental facilities.

References

- [1] A. Luo, M.O. Pekguleryuz, *J. Mater. Sci.* 29 (1994) 5259–5271.
- [2] A.A. Luo, *Int. Mater. Rev.* 49 (2013) 13–30.
- [3] E.G. Sieracki, J.J. Velazquez, K. Kabiri, SAE Technical Paper 960421 (1996).
- [4] L. Bichler, C. Ravindran, D. Sediako, *Can. Metall. Q.* 48 (2013) 81–89.
- [5] P. Bakke, K. Pettersen, H. Westengen, *JOM* 55 (2003) 46–51.
- [6] P. Bakke, H. Westengen, The role of rare earth elements in structure and property control of magnesium die casting alloys, in: S.N. Mathaudhu, A.A. Luo, N.R. Neelameggham, E.A. Nyberg, W.H. Sillekens (Eds.), *Essential Readings in Magnesium Technology*, Springer International Publishing, Cham, 2016, pp. 313–318.
- [7] S.G. Lee, G.R. Patel, A.M. Gokhale, A. Sreeranganathan, M.F. Horstemeyer, *Mater. Sci. Eng. A* 427 (2006) 255–262.
- [8] T. Rzychoń, A. Kiełbus, J. Cwajna, J. Mizera, *Mater. Charact.* 60 (2009) 1107–1113.
- [9] S.M. Zhu, J.F. Nie, M.A. Gibson, M.A. Easton, P. Bakke, *Metall. Mater. Trans. A* 43 (2012) 4137–4144.
- [10] J. Zhang, K. Liu, D. Fang, X. Qiu, D. Tang, J. Meng, *J. Mater. Sci.* 44 (2009) 2046–2054.
- [11] J. Zhang, S. Liu, Z. Leng, M. Zhang, J. Meng, R. Wu, *Mater. Sci. Eng. A* 528 (2011) 2670–2677.
- [12] M.A. Easton, S. Zhu, T.B. Abbott, M. Dargusch, M. Murray, G. Savage, N. Hort, M.A. Gibson, *Adv. Eng. Mater.* 18 (2016) 953–962.

- [13] S. Zhu, M.A. Easton, T.B. Abbott, J.F. Nie, M.S. Dargusch, N. Hort, M.A. Gibson, *Metall. Mater. Trans. A* 46 (2015) 3543–3554.
- [14] B.R. Powell, V. Rezhets, M.P. Balogh, R.A. Waldo, *JOM* 54 (2002) 34–38.
- [15] J. Zhang, P. Yu, K. Liu, D. Fang, D. Tang, J. Meng, *Mater. Des.* 30 (2009) 2372–2378.
- [16] S.M. Zhu, M.A. Gibson, J.F. Nie, M.A. Easton, T.B. Abbott, *Scr. Mater.* 58 (2008) 477–480.
- [17] Q. Yang, X. Liu, F. Bu, F. Meng, T. Zheng, D. Zhang, J. Meng, *Intermetallics* 60 (2015) 92–97.
- [18] S. Lv, Y. Li, F. Meng, Q. Duan, Q. Yang, X. Liu, J. Meng, *Comput. Mater. Sci.* 131 (2017) 28–34.
- [19] S. Zhu, M.A. Easton, T.B. Abbott, M.A. Gibson, J.F. Nie, *Adv. Eng. Mater.* 18 (2016) 932–937.
- [20] F. Meng, S. Lv, Q. Yang, P. Qin, J. Zhang, K. Guan, Y. Huang, N. Hort, B. Li, X. Liu, J. Meng, *J. Alloy. Compd.* 795 (2019) 436–445.
- [21] S.M. Zhu, T.B. Abbott, M.A. Gibson, J.F. Nie, M.A. Easton, *Mater. Sci. Eng. A* 656 (2016) 34–38.
- [22] S.M. Zhu, T.B. Abbott, M.A. Gibson, J.F. Nie, M.A. Easton, *Mater. Sci. Eng. A* 682 (2017) 535–541.
- [23] Q. Yang, K. Guan, B. Li, S. Lv, F. Meng, W. Sun, Y. Zhang, X. Liu, J. Meng, *Mater. Charact.* 132 (2017) 381–387.
- [24] P.F. Qin, Q. Yang, Y.Y. He, J.H. Zhang, J.S. Xie, X.R. Hua, K. Guan, *J. Meng, Rare Metals* 40 (2021) 2956–2963.
- [25] R. Zeng, Y. Chiu, I.P. Jones, *J. Alloy. Compd.* 579 (2013) 34–38.
- [26] H.Q. Ang, T.B. Abbott, S. Zhu, C. Gu, M.A. Easton, *Mater. Des.* 112 (2016) 402–409.
- [27] S. Lv, X. Lü, F. Meng, Q. Yang, X. Qiu, P. Qin, Q. Duan, J. Meng, *Mater. Sci. Eng. A* 773 (2020).
- [28] PANDAT Software for Thermodynamic Calculation and Kinetic Simulation, CompuTherm LLC, Middleton, WI 53562, USA.
- [29] M. Kunst, A. Fischersworing-Bunk, G. L'Esperance, P. Plamondon, U. Glatzel, *Mater. Sci. Eng. A* 510–511 (2009) 387–392.
- [30] T. Homma, S. Nakawaki, S. Kamado, *Scr. Mater.* 63 (2010) 1173–1176.
- [31] T. Homma, S. Nakawaki, K. Oh-ishi, K. Hono, S. Kamado, *Acta Mater.* 59 (2011) 7662–7672.
- [32] B. Backes, K. Durst, D. Amberger, M. Göken, *Metall. Mater. Trans. A* 40 (2009) 257–261.
- [33] S. Lamm, D. Matschkal, M. Göken, P. Felfer, *Mater. Sci. Eng. A* 761 (2019) 137964.
- [34] S.M. Zhu, M.A. Gibson, M.A. Easton, J.F. Nie, *Scr. Mater.* 63 (2010) 698–703.
- [35] N. Li, R. Osborne, B. Cox, D. Penrod, *SAE Technical Paper* 2005-01-0337 (2005).
- [36] B. Zhang, S. Gavras, A.V. Nagasekhar, C.H. Cáceres, M.A. Easton, *Metall. Mater. Trans. A* 45 (2014) 4386–4397.